THE GEOLOGICAL SOCIETY OF AMERICA®

Sources of Perennial Water Supporting Critical Ecosystems, San Pedro Valley, Arizona

CHRISTOPHER J. EASTOE[1,*]

Department of Geosciences, University of Arizona, Tucson, AZ 85719

Key Terms: ***Geohydrology, Base Flow, Groundwater, Stable Isotopes, Tritium, Arizona***

ABSTRACT

Stable O and H isotope data distinguish three sources for base flow in five reaches of the San Pedro River: (A) base flow and sub-flow from upstream reaches of the river; (B) bank storage derived from summer monsoon floodwater; and (C) water from the mountainous flanks of the river catchment. A and C support base flow in the sub-basin upstream of Sierra Vista. A, B, and C combine to support base flow near St. David. Source C in this area is ancient deep-basin groundwater. Source C dominates in Cascabel near Benson Narrows, with downstream additions from A. In Cascabel near Gamez Road, sources A and C combined to support base flow that had disappeared by 2019. Near Redington, source C appears to have operated through a limestone aquifer vulnerable to short-term drought. Groundwater sub-basins separated by impermeable sills in the riverbed are evolving into hydrologically separate sub-basins as base flow across the sills decreases. The decrease in base flow partly reflects regional long-term drought, which has been exacerbated by pumping. Additional groundwater demand from urban growth upstream of Benson is likely to cause further decline of base flow near St. David and Sierra Vista.

INTRODUCTION

The San Pedro River (SPR) rises in the Huachuca Mountains of southern Arizona, flows into northern Sonora, Mexico, returns to Arizona, and then flows north about 200 km to join the Gila River (Figure 1). Surface and subsurface water in the riparian zone supports a semi-continuous ribbon of riparian vegetation through the surrounding semiarid-to-arid landscape. Discontinuous reaches with perennial water furnish small but crucial amounts of water to local and migrating fauna. Since documentation began in 2007, most of the perennial reaches have declined in length (The Nature Conservancy, 2020). The decline has occurred concurrently with a drought of decadal timescale (Abatzoglu et al., 2017; WestWide Drought Tracker, 2019), but it probably also reflects overdraft of groundwater (Cordova et al., 2015; Gungle et al., 2017).

The river valley constitutes a corridor between forested terrains of the Sierra Madre Occidental in Mexico and the southern edge of the Colorado Plateau in the United States and lies close to the boundary between the Sonoran and Chihuahuan Deserts. Its location, in combination with the availability of water, has engendered rich faunal biodiversity. Vertebrates in the Upper San Pedro Valley (SPV) include 61 to 87 species of mammals, 100 species of breeding birds, 200 species of migrating birds, and 55 recorded reptiles and amphibians (Brand et al., 2009; Rosen, 2009; and Soycan et al., 2009). Maricopa Audubon Society (2020) lists "over 375" bird species recorded in the San Pedro Riparian National Conservation Area. Avian density in the riparian *Populus* forests is high: 431 ± 22 birds per 40 ha in the breeding season, and 1468 ± 92 birds per 40 ha during the spring migration, with the latter figure exceeding comparable avian density estimates on the Rio Grande and Colorado River by factors of 3.1 and 8.5, respectively (Brand et al., 2009). In the less-settled area north of Benson, AZ, the SPV is crossed by major wildlife corridors linking the "sky islands" of flanking mountain ranges. The SPV is therefore a high-priority area for conservation, a major aspect of which is preservation of surface and subsurface water in the riparian zone.

From the city of Sierra Vista to the Mexico-U.S. border (Figure 1), the valley has undergone high human population growth. Pressure for urban development between Sierra Vista and Benson is increasing (Arizona Daily Star, 2016). Such development inevitably leads to competition between human settlements and riparian plant and animal communities for scarce water resources. Preservation of surface water requires a clear understanding of sources of the perennial water.

Stable O and H isotope effects such as altitude effects and the damping of ranges of $\delta^{18}O$ and $\delta^{2}H$ in groundwater relative to precipitation provide means of identifying sources of base flow, locating

[1]Retired

*Corresponding author email: eastoe@email.arizona.edu

Downloaded from http://pubs.geoscienceworld.org/aeg/eeg/article-pdf/26/4/463/5196653/i1078-7275-26-4-463.pdf
by University of Arizona user

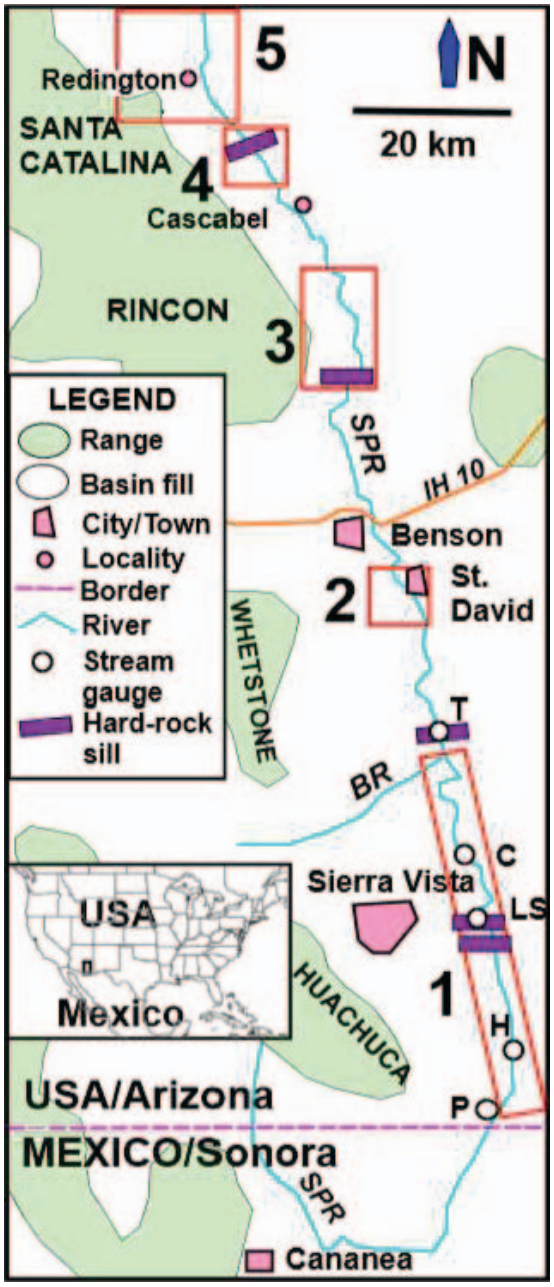

Figure 1. Location map showing study areas 1 to 5.

groundwater discharge zones, and relating sources and discharge to geology at a variety of scales. In small-area catchments, $<10^2$ km^2, isotope signals related to base flow may be masked by seasonal variation in $\delta^{18}O$ and δ^2H (Soulsby et al., 2000; Blumstock et al., 2015). In other cases, sources of base flow can be related to topographic features (Singh et al., 2016), deep groundwater in volcanic strata (Fujimoto et al., 2016), and storage in colluvium (Segura et al., 2019). In mesoscale catchments, 10^2 to 10^4 km^2, isotope evidence yielded little insight in the Dee River watershed, Scotland (Tetzlaff and Soulsby, 2008), but identified baseflow sources in higher-permeability strata of catchments in Luxemburg (Pfister et al., 2017) and Oregon, United States (Nickolas et al., 2017). In the Willamette River catchment, Oregon, base flow in dry years is sustained by groundwater stored in high-permeability volcanic strata of the Cascade Range (Tague and Grant, 2004; Brooks et al., 2012). Larger catchments, $>10^5$ km^2, include rivers that flow from well-watered source regions into desert, where isotope changes are controlled by evaporation, e.g., the Barwon-Darling River, Australia (Hughes et al., 2012), and the Colorado River, United States (Guay et al., 2006). In the upper Rio Grande catchment, United States, discharge of groundwater into the river was not detected in isotope data where the river exits alluvium-filled grabens, but it was visible as stepwise increases in Cl^- concentration and Cl^-/Br^- ratios (Phillips et al., 2003; Hogan et al., 2012).

The SPR catchment, about 1.2×10^4 km^2, differs from catchments of comparable size mentioned above in that the river is ephemeral over much of its length (The Nature Conservancy, 2020). Between December and June, source points of base flow are readily identified at the heads of reaches with perennial water. The sources of base flow and the relationship of perennial water in successive reaches are matters of relevance to management of the river. This article reviews current understandings of the geology and hydrology of the SPV between the Mexico-U.S. border and Redington, Arizona (Figure 1), and examines new and existing isotope data with the aim of providing an improved understanding of water sources for future management of the SPV.

BACKGROUND

Study Area

This study considered a 130 km length of the SPV between the U.S.-Mexico border (1410 meters above sea level [masl]) and Redington, Arizona (980 masl). Within this interval, five river segments (areas 1 to 5 of Figures 1 and 2) have had perennial water, i.e., base flow in the driest seasons, for part or all of the interval 2000–2019. Watershed altitudes extend to 2700 masl in flanking mountain ranges.

The climate is semiarid, except above 2000 masl. Average annual rainfall at representative stations is 355 mm at Sierra Vista, 288 mm at Benson, 338 mm at Cascabel, and 345 mm at Redington, while at 2345 masl in the Santa Catalina Mountains, the average is 762 mm (Western Regional Climate Center, 2019). Precipitation totals vary greatly from year to year. Two wet seasons occur: a season of orographic rain or snow

Downloaded from http://pubs.geoscienceworld.org/aeg/eeg/article-pdf/26/4/463/5196653/i1078-7275-26-4-463.pdf
by University of Arizona user

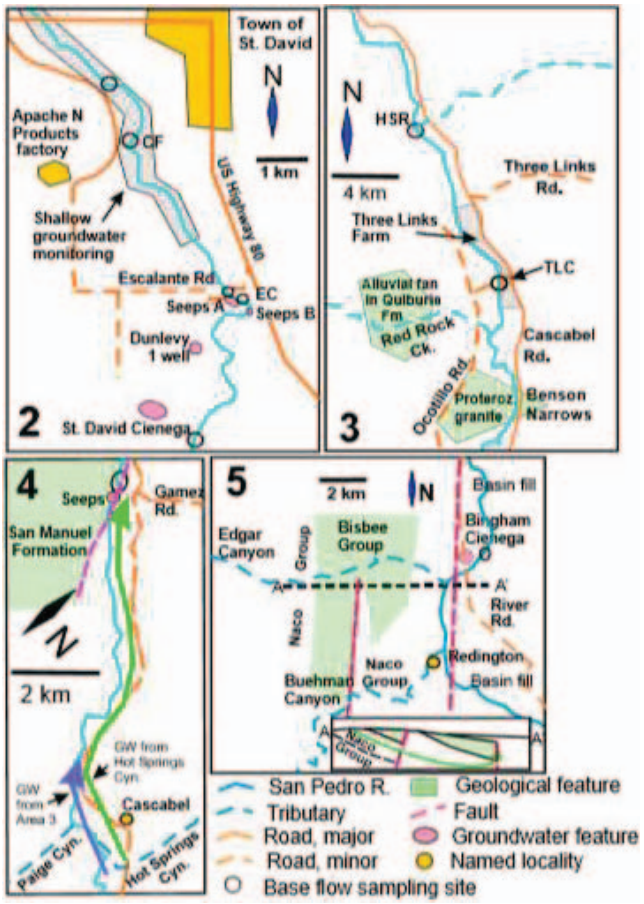

Figure 2. Detailed maps of study areas 2 to 5, indicated by bold numerals. Site name abbreviations in area 3 map: TLC = Three Links Crossing; HSC = Heaven Sent Ranch; UTW = upstream of Teran Wash; DTW = downstream of Teran Wash.

from Pacific fronts during winter and spring, and a season of convective precipitation from the North American Monsoon between late June and September. In some years, tropical depressions provide heavy rains in September and October. June–October precipitation makes up about 70 percent of precipitation south of Sierra Vista, and about 60 percent of that north of Benson (Western Regional Climate Center, 2019).

Along the river channel, riparian forest, mainly *Populus*, *Salix*, *Baccharis*, and invasive *Tamarix*, forms a discontinuous strip up to a few hundred meters wide; its presence and width depend on availability of shallow groundwater. Mesquite (*Prosopis*) woodland occupies higher terraces, commonly forming bands tens to hundreds of meters wide. Much mesquite woodland has been cleared for agriculture. Dry basin slopes are occupied by Sonoran Desert vegetation, commonly stunted *Prosopis*, *Larrea*, *Acacia*, *Opuntia*, *Cylindropuntia*, and *Yucca*, along with forbs, grasses, and annuals. Vegetation on lower mountain slopes is dominated by *Quercus*, *Juniperus*, and *Arctostaphylos*, and by *Pinus* at higher elevations.

Geology and Hydrogeology

The SPV is a faulted trough within the extensional Basin and Range Province (Fenneman, 1931). Tectonic extension began about 20 Ma, leading initially to the deposition of granitic detritus forming the San Manuel Formation in the northern part of the study area (Dickinson, 1991, 2002). From 11 Ma, deep extensional basins opened within the study area. Geologic evolution of the SPV differs north and south of the Benson Narrows (Figure 2), a valley-wide block of Proterozoic granite. To the north, internal drainage prevailed between 11 and 5 Ma, resulting in the accumulation of alluvial, fluvial, and lacustrine/evaporitic facies of the Quiburis Formation (Dickinson, 1998, 2003). South of the Benson Narrows, exposed basin fill in the Benson–St. David area (Figure 2) consists of alluvial/fluvial siltstone and mudstone with lesser lacustrine facies, named the St. David Formation of Pliocene to Pleistocene age (Gray, 1965). Beneath the St. David Formation, an up to 200 m section of lacustrine or wetland clay-rich sediment overlies about 200 m of coarser clastics, both of undetermined age (Dickinson et al., 2010a, 2010b). Clay-rich sediment also accumulated in the basin upstream of Sierra Vista (Pool and Dickinson, 2007).

Dickinson (1998) proposed that an external, integrated drainage system comprising the ancestral San Pedro and Gila Rivers developed north of the Benson Narrows by 5 Ma, leading to subsequent erosion of much of the Quiburis Formation. Drainage from south of the Benson Narrows into the ancestral SPR had developed by the mid-Pliocene. The rate of erosion of the St. David Formation in the Benson area increased greatly during the Pleistocene.

Except where it crosses impermeable sills, the present riverbed lies within a band of Holocene fluvial and wetland sediments up to 1500 m wide, partly concealed by younger alluvium (Cook et al., 2010). The sediments occupy a trench cut into basin-fill sediments since about 20 ka (Huckleberry et al., 2009). Starting possibly in the 1850s in the Cascabel area (Hereford and Betancourt, 2009), the river excavated an entrenched channel up to 6 m deep in the trench sediments. Late nineteenth-century entrenchment was a regional phenomenon in Arizona and neighboring areas (Bryan, 1925), possibly resulting from climate change or from human-related activities such as removal of beavers and overgrazing (Hereford and Betancourt, 2009). Six synchronous cycles of entrenchment and valley filling have been documented across southeastern Arizona in the last

Downloaded from http://pubs.geoscienceworld.org/aeg/eeg/article-pdf/26/4/463/5196653/i1078-7275-26-4-463.pdf
by University of Arizona user

4,000 years (Waters and Haynes, 2001), suggesting a natural, cyclic cause.

Basin-fill sediments constitute the productive aquifers of the SPV. Principal hydrogeological features of the basin are as follows.

(1) The well-watered mountain areas, where winter snow may accumulate, provide runoff that recharges alluvium along the basin flanks and at times reaches the SPR.
(2) Coarse clastic sediments along the basin flanks, locally fining towards the basin axis, make up a regional, unconfined aquifer where no thick clay unit is present (e.g., Baillie et al., 2007; Hopkins et al., 2014).
(3) Thick clay-rich units near Benson and south of Sierra Vista confine groundwater, locally under flowing artesian conditions, in underlying coarse clastic sediments. In the Benson area, confined-aquifer groundwater is ancient; 19 samples for which data are available contained 1 to 33 pMC. Of 16 samples with tritium analyses, 14 contained less than 1 TU (Hopkins et al., 2014).
(4) The post–20 ka trench sediments, including clastic units, are less consolidated and more permeable than the sediment into which the trench was cut.
(5) Impermeable sills in the riverbed (Figure 1) consist of Cretaceous igneous and sedimentary rock in area 1 near Sierra Vista, Proterozoic granite in area 3 at the Benson Narrows, and an argillaceous unit of the San Manuel Formation in area 4 (Figure 2). Little or no trench sediment is present at the sills, but unconsolidated Holocene fluvial sediment occurs beneath the river.
(6) Parallel paleochannels act as groundwater conduits within the trench sediments. Such channels were identified near Sierra Vista (Waters and Haynes, 2001) and were inferred near Cascabel (Eastoe and Clark, 2018).

The post–20 ka trench sediments constitute the most productive aquifers north of the Benson Narrows, where clay-rich lenses confine groundwater within underlying clastic sediment of the trench (Eastoe and Clark, 2018). South of the Benson Narrows, much groundwater is extracted from the coarse clastic basin-fill alluvium beneath broader bodies of clay-rich sediment (Hopkins et al., 2014; Pool and Dickinson, 2007). In both areas, local shallow riparian aquifers are perched atop the clay-rich sediments (Baillie et al., 2007; Huckleberry et al., 2009; MacNish et al., 2009; and Eastoe and Clark, 2018).

Recharge to basin-fill alluvium is probably focused along major tributary washes, occurring mainly from mountain runoff at or near the mountain fronts (Wahi et al., 2008; Hopkins et al., 2014). Local recharge occurs from the SPR to shallow riparian aquifers (Baillie et al., 2007; Hopkins et al., 2014; and Eastoe and Clark, 2018). Near Sierra Vista, diffuse recharge may not reach the regional aquifer from areas between streambeds (Glenn et al., 2015).

Previous Water Isotope Studies

In the SPV near Sierra Vista, measurements of stable O and H isotopes and tritium in precipitation were made from 2000 to 2003 (Coes and Pool, 2007), and in 2004–2005 (Baillie et al., 2007). Coes and Pool (2007) used tritium data to determine infiltration rates beneath tributary washes near Sierra Vista. Wahi et al. (2008) and Baillie et al. (2007) used stable water isotopes, tritium, ^{14}C, and major ion concentrations to establish the relationships among mountain-block groundwater in the Huachuca Mountains, basin groundwater, and discharge into the SPR. Gungle et al. (2017) summarized long-term water isotope data sets collected at five U.S. Geological Survey stream gauge sites on the SPR south of Tombstone, AZ (Figure 1). Their data documented: (1) an increase in $\delta^{18}O$ in base flow from 2000 to 2012, consistent with a decreasing fraction of local groundwater; and (2) discharge of mountain-derived groundwater into certain reaches of the SPR under base-flow conditions. Near Benson, Hopkins et al. (2014) used stable water isotopes, tritium, ^{14}C, and major ion concentrations to determine groundwater types and residence times in shallow riparian, confined sub-clay, and unconfined alluvial aquifers. In the Cascabel area, Eastoe and Clark (2018) used stable water isotopes and tritium to distinguish groundwater of different sources and residence times.

METHODS

Water samples for isotope measurement were collected from surface flows, springs, and wells in continual use. New isotope data (Supplemental Table S1) were measured at the Environmental Isotope Laboratory, University of Arizona. Stable O and H isotope measurements were made on a Finnigan Delta S dual-inlet mass spectrometer with an automated CO_2 equilibrator (for O) and an automated Cr-reduction furnace (for H). Results are expressed in the usual delta notation, e.g.,

$$\delta^{18}O \text{ or } \delta^{2}H = 1000 \left\{ \frac{R(sample)}{R(standard)} - 1 \right\} ‰, \quad (1)$$

where $R = {}^{18}O/{}^{16}O$ or ${}^{2}H/{}^{1}H$. Analytical precisions (1σ) are 0.08‰ for O and 0.9‰ for H.

Tritium was measured by liquid scintillation counting in a Quantulus 1220 spectrometer. Samples of

Downloaded from http://pubs.geoscienceworld.org/aeg/eeg/article-pdf/26/4/463/5196653/i1078-7275-26-4-463.pdf
by University of Arizona user

Table 1. *Simplified water budgets in three sub-basins of the San Pedro Valley after Cordova et al. (2015) and Gungle et al. (2017).*

Sub-Basin	Year	Inflow (hm^3/yr)	ET (hm^3/yr)	HD (hm^3/yr)	ET/Inflow (%)	HD/Inflow (%)
Sierra Vista*	2012	20.3	15.0	15.0	74	74
Benson#	2010	20.0	17.1	9.1	86	46
Cascabel to Redington§	2010	13.8	12.2	2.8	88	20

ET = evapotranspiration; HD = human demand.
*Sierra Vista, AZ, i.e., area 1 of this study.
#Charleston to Benson Narrows, including area 2 of this study.
§Benson Narrows to Redington, including areas 3 and 4 of this study.

0.19 L were enriched by electrolysis and measured with a detection limit of 0.6 TU. Results are expressed in tritium units (TU); 1 TU corresponds to 1 tritium atom per 10^{18} hydrogen atoms. For calibration, international standards Vienna standard mean ocean water (VSMOW), standard light Antarctic precipitation (SLAP), and NBS-4361C were used. Values of $\delta^{18}O$ and $\delta^{2}H$ are expressed relative to VSMOW.

RESULTS

SPR Floodwater

Stable O and H isotope data from four gauge sites in area 1 (Gungle et al., 2017) and from area 3 (Table 1; see locations in Figures 1 and 2) are shown in Figure 3; the data do not represent all flood events during the intervals indicated. The ranges at both sites are broad, reflecting the isotopic heterogeneity of individual rain events in the region (Eastoe and Dettman, 2016). Low values of $\delta^{18}O$ and $\delta^{2}H$ from area 3 between September 19 and October 4, 2014, followed heavy rain generated by hurricane Odile; in Tucson, associated rain had ($\delta^{18}O$, $\delta^{2}H$) values of (−15.2‰, −125‰), evolving to (−9.3‰, −73‰).

Shallow Riparian Groundwater

Data for area 1 form a linear trend with a slope of 5.6, with two clusters corresponding to gaining and losing reaches (Figure 4), and these data were interpreted to indicate mixing between summer runoff that dominates recharge in losing reaches and basin groundwater containing winter recharge from the Huachuca Mountains in gaining reaches (Baillie et al., 2007).

Data for areas 2 and 3, including Benson (Hopkins et al., 2014) and the riverbed near the Apache Nitrogen factory (Beilke, 2006), are from losing reaches of the river and plot with the losing-reach data of area 1. The data form a linear trend having a slope of 3.4 (omitting one outlier that probably represents

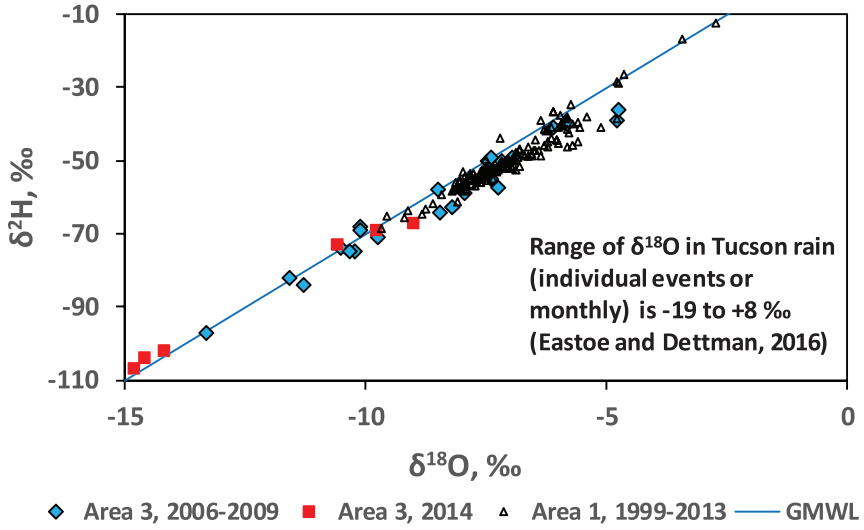

Figure 3. $\delta^{2}H$ vs. $\delta^{18}O$ values for floodwater in the San Pedro River. Data for area 3, 2014, are for floodwater following rain associated with Hurricane Odile. GMWL = global meteoric water line.

Downloaded from http://pubs.geoscienceworld.org/aeg/eeg/article-pdf/26/4/463/5196653/i1078-7275-26-4-463.pdf
by University of Arizona user

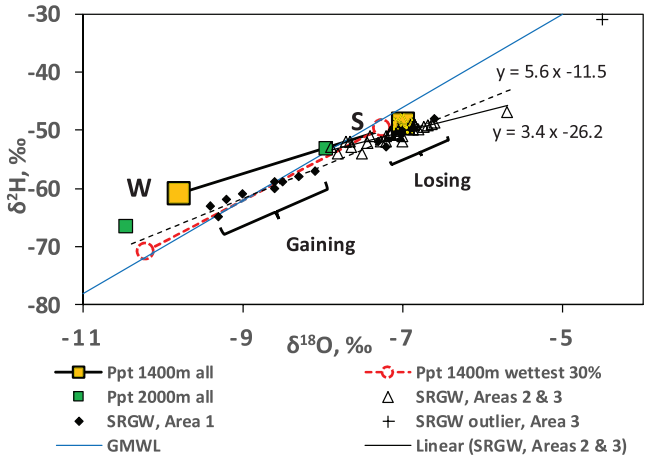

Figure 4. δ^2H vs. δ^{18}O values for shallow riparian groundwater (SRGW) in the floodplain of the San Pedro River. Also shown are estimated seasonal weighted mean isotope data for precipitation (Ppt), based on data for Tucson Basin with altitude corrections (Eastoe and Dettman, 2016). "Ppt 1400 m all" signifies means for all precipitation at an altitude of 1400 masl. "Ppt 1400 m wettest 30%" signifies means for precipitation in the wettest 30% of months at an altitude of 1400 masl. Data for area 1 are distinguished as belonging to gaining and losing reaches of the river, following Baillie et al. (2007). GMWL = global meteoric water line.

recharge from a particular flood event) and appear to define an evaporation trend originating near the summer end member of a modified local meteoric water line (LMWL) defined by amount-weighted means for precipitation falling during the wettest 30 percent of months. Recharge to basin fill in southern Arizona occurs mainly during the wettest months (Eastoe and Towne, 2018). The modified LMWL was calculated for an altitude of 1400 masl using precipitation data and isotope lapse rates for Tucson Basin (Eastoe and Dettman, 2016; Eastoe and Wright, 2019). Modified LMWLs up to 1700 masl differ little from the LMWL for 1400 masl. Shallow riparian groundwater (SRGW) in losing reaches of areas 1, 2, and 3 represents isotopically integrated bank storage of summer floodwater, consistent with the near absence of winter floods (Figure 7 of Cordova et al., 2015), and it has undergone evaporation since integration, suggesting repeated discharge and infiltration in the river channel.

Area 1

The data (Figure 5) are from Gungle et al. (2017), and they represent samples collected between December and June (in order to avoid monsoon runoff) at four U.S. Geological Survey stream gauging stations: Hereford, Lewis Springs, Charleston, and Tombstone (Figure 1). For each site, the (δ^{18}O, δ^2H) values define a statistically significant linear trend, which is compared with data for groundwater in the basin alluvium between the Huachuca Mountains and the SPR (Wahi et al., 2008). The trend with highest slope, 5.9, is for the Lewis Springs site, and it represents the river reach upstream of that site. The slope is like that of the mixing trend for SRGW in area 1 (Figure 4) and indicates mixing between basin groundwater and summer runoff. The lowest slope, 3.7, is for the Tombstone site, and it is generated by evaporation of base flow from the Charleston site, 14 km upstream. At the Hereford and Charleston sites, intermediate slopes suggest combinations of mixing and evaporation in the reaches upstream of those sites.

Area 2

Along the axis of the SPV in area 2, a unit of impermeable clay-rich sediment 200 m thick, locally termed the Benson Clay, separates a shallow riparian aquifer from a deep, confined aquifer (Hopkins et al., 2014). Warm (23–26°C), flowing artesian groundwater discharges through the Benson Clay at the uncapped Dunlevy well and within the St. David Cienega (Figure 2). Springs in the bed of the SPR up to 100 m upstream of Escalante Crossing (Seeps A in Figure 2) apparently discharge water that moves upward through the Benson Clay. A second set of seeps (Seeps B, active in 2014 and 2015, but dry in February 2018) discharges water 1–2 m above the riverbed from a low cliff face about 500 m upstream of Escalante Crossing. This water flows along the top surface of the Benson Clay, probably in a buried paleochannel separate from the present river course. A perennial reach commonly begins at these seeps and at times continues beyond the Highway 80 bridge.

Confined-aquifer groundwater in the Benson–St. David area ranges in isotope composition (Figure 6) from (δ^{18}O, δ^2H) = (−7.4‰, −49‰), similar to shallow riparian groundwater, to (−11.8‰, −85‰). Higher (δ^{18}O, δ^2H) values are observed near the SPR (Hopkins et al., 2014). The least-evaporated samples from St. David Cienega, near (−8.3‰, −60‰), differ from confined groundwater near the river.

Groundwater from atop the Benson Clay (Seeps B) has (δ^{18}O, δ^2H) values consistent with base flow measured at the Tombstone gauge (Figure 5D). Groundwater from Seeps A changed in (δ^{18}O, δ^2H) values between 2014 and 2018. In 2018, three seeps were discharging water that plots as shallow riparian groundwater. In 2015, a sample from one of the seeps, marked by growth of orange algae, yielded (−8.9‰, −64‰), and in 2014, a nearby seep was discharging water with (−7.5‰, −55‰). A riverbed seep sampled near Curtis Station in 2006 gave (−8.9‰, −66‰).

Four samples of base flow from the river plot in a linear array between shallow riparian groundwater

Downloaded from http://pubs.geoscienceworld.org/aeg/eeg/article-pdf/26/4/463/5196653/i1078-7275-26-4-463.pdf
by University of Arizona user

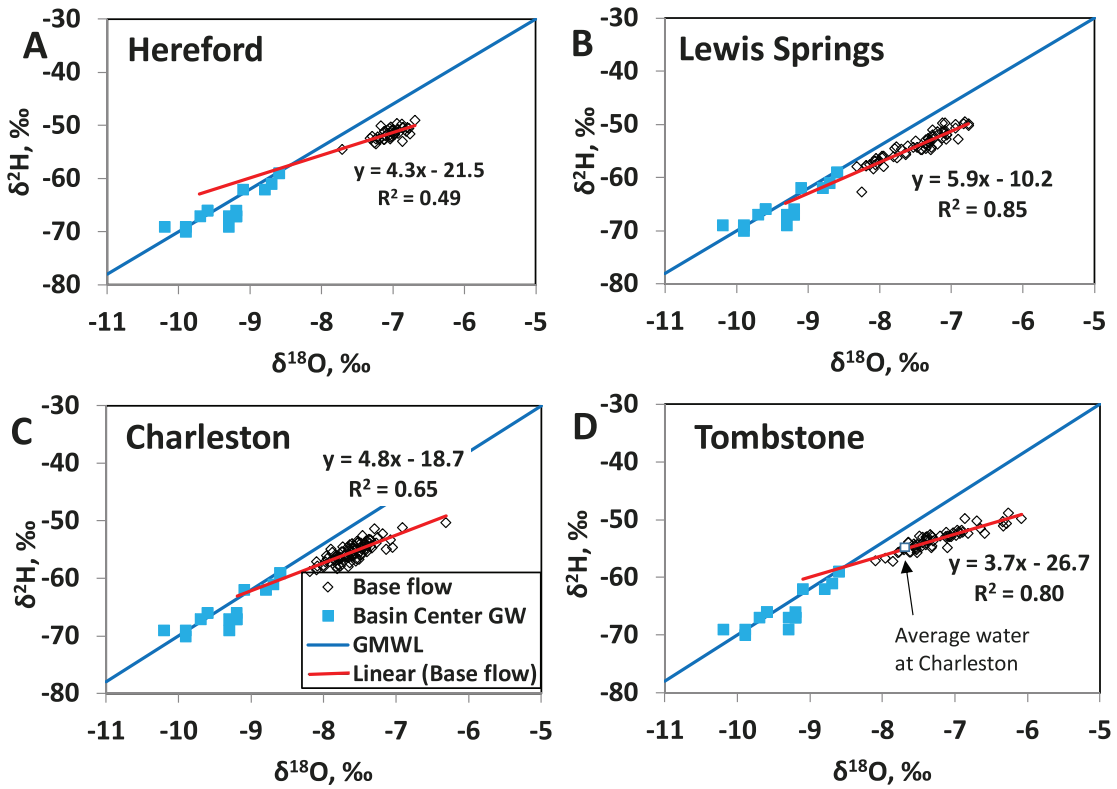

Figure 5. δ^2H vs. $\delta^{18}O$ values for base flow in area 1, corresponding to sampling between December and June over several years at four stream gauge sites (Gungle et al., 2017), and groundwater in the central part of the alluvial basin (Baillie et al., 2007; Wahi et al., 2008). GMWL = global meteoric water line. $P < 0.0001$ for all correlation coefficients R.

and Tombstone gauge base flow. At least four sources of water contribute to base flow in area 2: (1) SRGW matching the evaporation trend of Figure 4; (2) base flow matching that from the Tombstone gauge (Figure 5); (3) confined-aquifer discharge with low values of ($\delta^{18}O$, δ^2H), e.g., (−8.9‰, −64‰); and (4) apparent confined-aquifer discharge with isotope composition close to that of bank storage. The contributions of (2) and (3) cannot be distinguished in Figure 6 because the data are close to collinear. Discharge of type (4) is likely to be masked by bank storage. The change in isotope composition at Seeps A is discussed below. The confined aquifer appears to be compartmentalized in isotope composition beneath area 2, yielding water of different isotope composition at neighboring sites (Seeps A, St. David Cienega, Dunlevy Wells, and a number of supply wells near St. David).

Type (4) water from wells near the SPR south of St. David (Hopkins et al., 2014; data reproduced in Supplemental Table S1) contains 10 to 20 pMC. It resembles confined-aquifer groundwater to the east of the SPR (Hopkins et al., 2014) and was probably recharged at the eastern flanks of the basin. It is not river water drawn recently into the confined aquifer as a result of pumping near St. David.

Area 3

The sub-basin in this area is separated from the sub-basin upstream by the granite sill at the Benson Narrows (Figure 1). Basin-fill sediment in area 3 consists mainly of semi-consolidated conglomerate of the Quiburis Formation. The river channel is confined to the post–20 ka trench, which is filled to a depth of at least 40 m with fluvial and clay-rich wetland or lacustrine sediments (Eastoe and Clark, 2018). The clay-rich sediments are present in the post–20 ka trench throughout area 3 (Cordova et al., 2015), forming impermeable lenses that separate a thin layer of active fluvial deposits from deeper gravel and sand deposits. A shallow riparian aquifer, possibly discontinuous, is perched above the clay-rich units, and a principal aquifer, continuous with a less-productive regional aquifer in the Quiburis Formation, occurs below the clay-rich unit. Recharge in area 3 consists of about-equal amounts of winter and summer precipitation from the wettest 30 percent (approximately) of months (Eastoe and Towne, 2018).

Base flow originates consistently near the confluence of Red Rock Creek with the SPR. In early 2007, base flow extended north to site DTW (Figure 2). Since

Downloaded from http://pubs.geoscienceworld.org/aeg/eeg/article-pdf/26/4/463/5196653/i1078-7275-26-4-463.pdf
by University of Arizona user

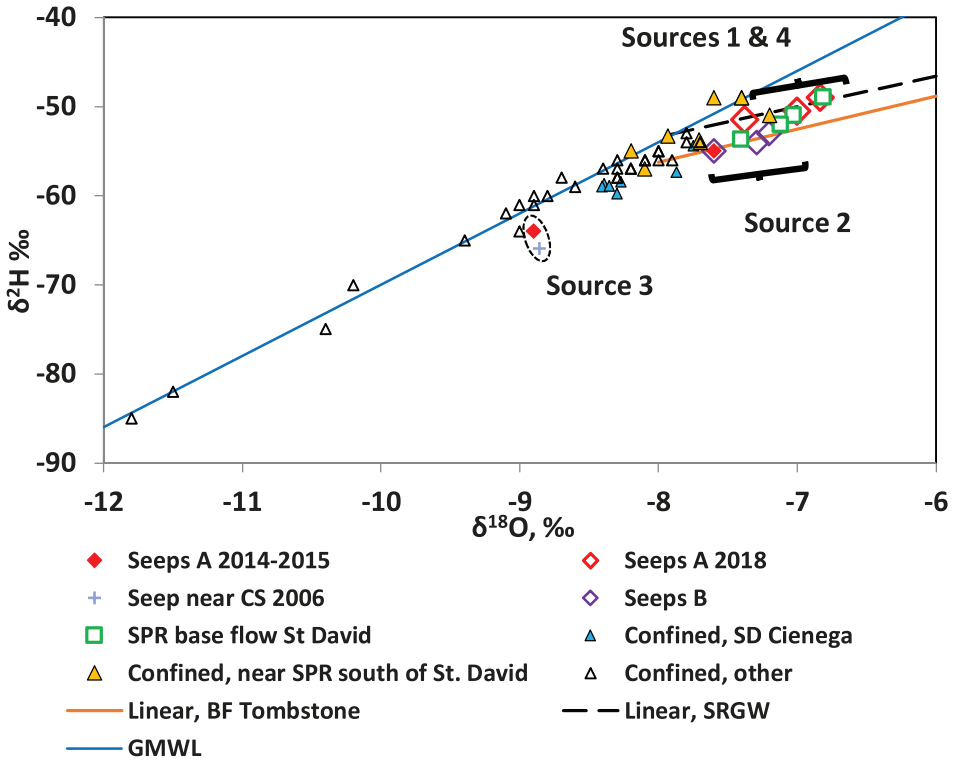

Figure 6. δ^2H vs. $\delta^{18}O$ values for area 2, showing data for: base flow in the San Pedro River (SPR); groundwater seeping into the riverbed; groundwater from the confined aquifer in basin alluvium, sampled from water supply wells (Hopkins et al., 2014) and at St. David Cienega (this study). Linear trends are from Figure 3 (shallow riparian groundwater, SRGW) and Figure 5 (base flow, BF, at Tombstone). CS = Curtis Station. GMWL = global meteoric water line. Locations are shown in Figure 2.

spring 2007, base flow has not extended beyond site UTW, and by June 2018, it had contracted to about 3 km beginning at Red Rock Creek (The Nature Conservancy, 2020). From 2007 to 2014, base flow at site TLC (location shown in Figure 2) commonly had ($\delta^{18}O$, δ^2H) near (−8.2‰, −59‰), and a tritium content of 1.0–1.7 TU (five of six samples; see Supplemental Table S1). In 2007–2009, base flow at downstream sites HSR, UTW, and DTW had a broader range of ($\delta^{18}O$, δ^2H). Values lower than those at TLC may result from local discharge of groundwater. Samples with higher values plot in an array that diverges from the global meteoric water line with increasing distance downstream and incorporate some evaporated irrigation reflux (originally groundwater of isotope composition like that of base flow at TLC). Samples from site DTW form a linear trend of slope 2.7, which could be an evaporation trend, but the slope is lower than usual for southern Arizona (Eastoe and Towne, 2018). A more nuanced explanation might involve progressive evaporation of base flow from TLC and mixing with SRGW (Figure 4). The downstream increase of tritium to 2.1–2.4 TU at site HSR (Table 1) is consistent with the latter suggestion.

Base flow at site TLC resembles neither SRGW nor confined groundwater immediately upstream of the Benson Narrows (Figure 7). The ($\delta^{18}O$, δ^2H) values of the base flow resemble those in groundwater associated with nearby catchments of similar elevation on the east flank of the sub-basin (Eastoe and Clark, 2018).

Area 4

Volcanic-derived conglomerate of the San Manuel Formation is faulted against fluvial/alluvial conglomerate of the Quiburis Formation in this area. Post–20 ka sediments fill a trench 100–300 m wide incised into the San Manuel Formation near the fault (Cook et al., 2010), except where an outcrop of impermeable, argillaceous beds of the San Manuel Formation occurs in the riverbed (32.3395°N, 110.4176°W). A cluster of seeps occurs 200–300 m upstream of that outcrop. Base flow, here termed the Gamez Road interval, extended about 200 m from the seeps in early 2014, but by June 2019, it had disappeared (The Nature Conservancy, 2020).

Eastoe and Clark (2018) provided evidence for parallel streams of groundwater of distinctive isotope

Downloaded from http://pubs.geoscienceworld.org/aeg/eeg/article-pdf/26/4/463/5196653/i1078-7275-26-4-463.pdf
by University of Arizona user

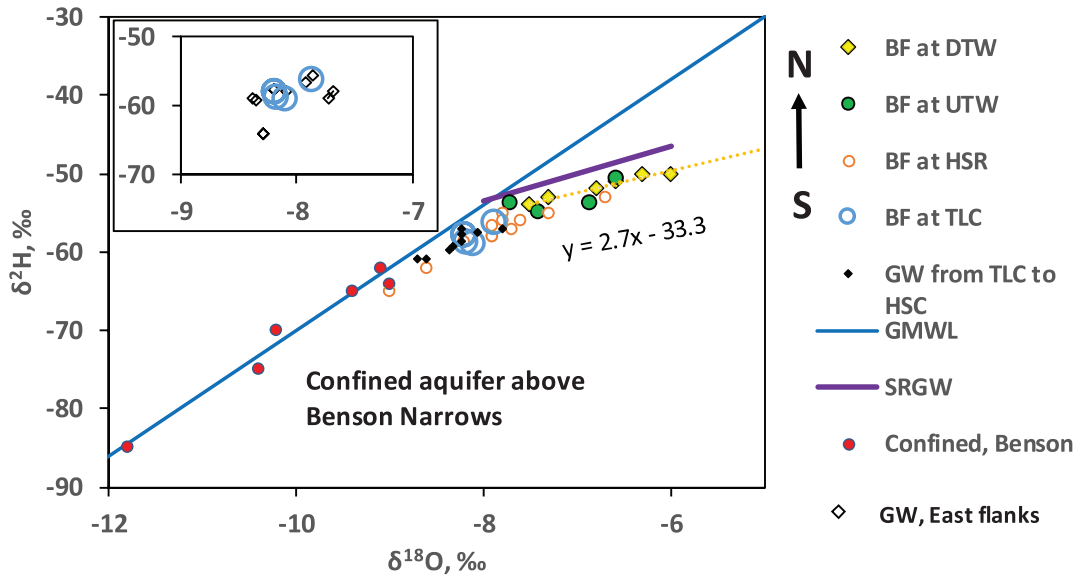

Figure 7. δ^2H vs. $\delta^{18}O$ values for area 3. Inset shows detail of Three Links Crossing (TLC) samples. BF = base flow, GW = groundwater, GMWL = global meteoric water line, SRGW = shallow riparian groundwater. Site name abbreviations (cf. Figure 2, area 3): TLC = Three Links Crossing; HSC = Heaven Sent Ranch; UTW = upstream of Teran Wash; DTW = downstream of Teran Wash.

composition, probably localized within paleochannels of the river between Hot Springs Canyon and the Gamez Road base-flow interval. To the east of the SPR, samples from numerous wells delineate an aquifer in which groundwater is derived from Hot Springs Canyon. Close to the river channel, a stream of groundwater like that in area 3 has been traced as shown in Figure 2; no well samples are available further downstream. Groundwater from Paige Canyon is a third distinctive type (Figure 8) that has not been traced beyond the end of Paige Canyon. Of three seep samples taken in March 2014 ("Unnamed Spring" in Supplemental Table S1), two resemble groundwater from Hot Springs Canyon, and one may be a mixture of groundwater from Hot Springs Canyon and area 3 (Figure 8). Base flow sampled at its downstream limit in March 2014 consisted mainly of groundwater from area 3. In November 2014, the seeps were discharging bank storage from the large flood generated by Hurricane Odile in September 2014.

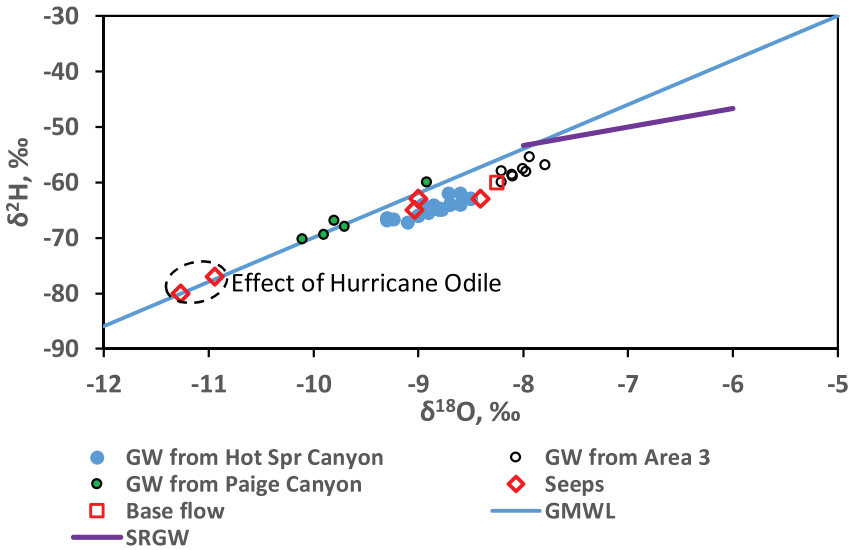

Figure 8. δ^2H vs. $\delta^{18}O$ values for area 4. GW = groundwater, GMWL = global meteoric water line, SRGW = shallow riparian groundwater.

Downloaded from http://pubs.geoscienceworld.org/aeg/eeg/article-pdf/26/4/463/5196653/i1078-7275-26-4-463.pdf
by University of Arizona user

Area 5

Holocene fluvial sediments in the post–20 ka trench broaden to a width of 1 km in this section of the SPV and are flanked on both sides by a further 2 km of Pleistocene alluvium (Cook et al., 2010) overlying lacustrine facies of the Quiburis Formation (Dickinson, 2003). Edgar and Buehman Canyons, both draining high elevations of the Santa Catalina Mountains, join the SPR near Redington, and upstream of Bingham Cienega, there is a spring-fed wetland 0.4 km north of the confluence of Edgar Canyon. Lower reaches of both canyons intersect the Buehman Canyon tilt block (Dickinson, 2003), consisting largely of east-dipping late Paleozoic limestone and Cretaceous shale and phyllite (Bykerk-Kaufmann, 1990). Base flow was observed in the SPR adjacent to Bingham Cienega between 1998 and 2001; since 2001, base flow has been absent.

In Figure 9, values of ($\delta^{18}O$, $\delta^{2}H$) from Bingham Cienega and base flow in the adjacent SPR are compared with data for groundwater from areas 3 and 4 (which supports base flow in area 4), and for surface water and groundwater from Edgar and Buehman Canyons. The following observations are offered: (1) base flow and spring water at Bingham Cienega are closely similar in isotope composition; (2) base flow has lower values of ($\delta^{18}O$, $\delta^{2}H$) than groundwater from area 3 and from Hot Springs Canyon in area 4; (3) water in Edgar Canyon is isotopically similar to groundwater associated with Paige Canyon; (4) three samples of water in Buehman Canyon on average have higher ($\delta^{18}O$, $\delta^{2}H$) values and appear to be more subject to evaporation than water from Edgar Canyon. Samples from base flow, Bingham Cienega, and Buehman Canyon contained 4.5, 4.0, and 5.0 TU, respectively, in June 2001.

Bingham Cienega and adjacent base flow appear to share a common source of recharge that was at most 5 years old in 2001 relative to average Tucson rainwater containing 5.3 TU (Eastoe et al., 2011). Water from the seeps at Gamez Road (area 4) cannot account for base flow at Bingham Cienega without addition of water with lower ($\delta^{18}O$, $\delta^{2}H$). Such water could originate from Edgar, Buehman, or Paige Canyons. Of these, Edgar and Buehman Canyons are the more likely because they are closer to the cienega. Water from Paige Canyon resembles that in Edgar Canyon because of source areas at altitudes above 2000 masl in each case. A mixture of water from Edgar and Buehman Canyons could account for water in base flow and Bingham Cienega.

DISCUSSION

Sills and Sub-Basins

Sills of impermeable rock near Sierra Vista, at the Benson Narrows, and near Gamez Road divide the study area into four hydrologic sub-basins. Prior to

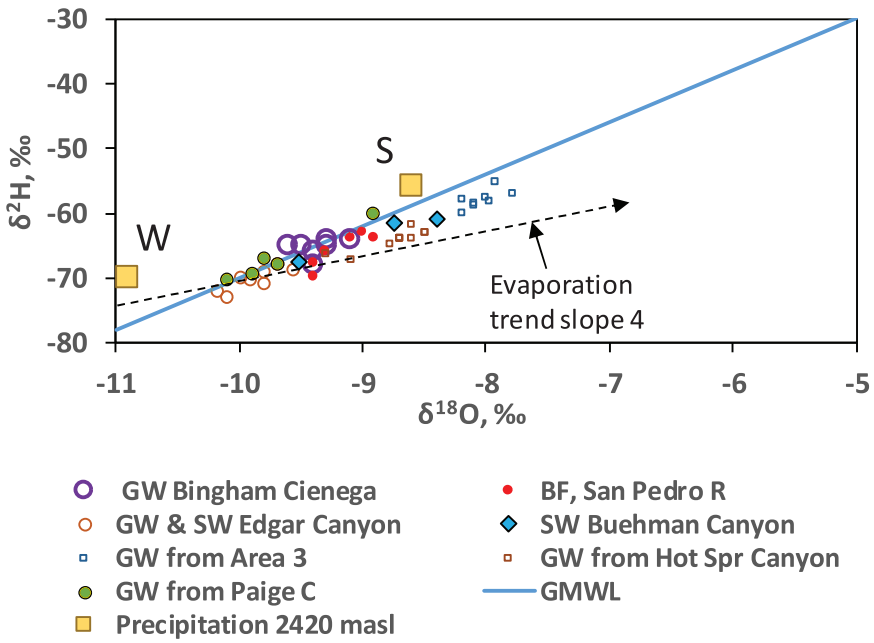

Figure 9. $\delta^{2}H$ vs. $\delta^{18}O$ values for area 5. GW = groundwater, SW = surface water, GMWL = global meteoric water line. Precipitation 2420 masl points show amount-weighted mean winter (W) and summer (S) means for an altitude of 2420 masl in the Santa Catalina Mountains (Eastoe and Wright, 2019).

Downloaded from http://pubs.geoscienceworld.org/aeg/eeg/article-pdf/26/4/463/5196653/i1078-7275-26-4-463.pdf
by University of Arizona user

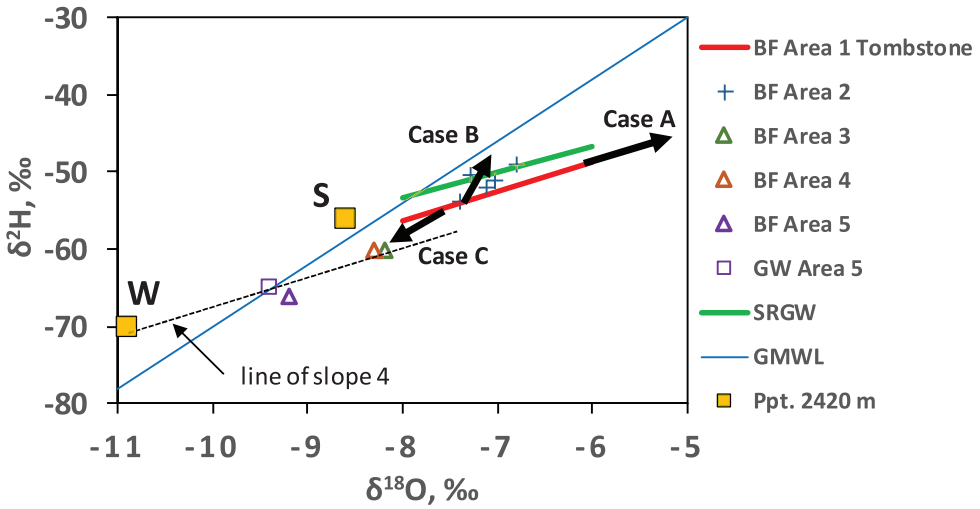

Figure 10. δ^2H vs. $\delta^{18}O$ summary diagram for base flow throughout the study area. Bold black arrows indicate isotope evolution corresponding to cases A, B, and C as discussed in the text. BF = base flow, GW = groundwater, GMWL = global meteoric water line, SRGW = shallow riparian groundwater. Ppt 2420 points show amount-weighted mean winter (W) and summer (S) means for an altitude of 2420 masl in the Santa Catalina Mountains (Eastoe and Wright, 2019).

development, groundwater would have crossed each sill as base flow or sub-flow through fluvial sediment in the post–20 ka trench. Observations near the Benson Narrows ("Shallow Riparian Groundwater" section) indicate no base flow for many years, consistent with overdraft of groundwater in the Benson–St. David area upstream of the sill (Cordova et al., 2015). At the Charleston gauge (Figure 1), base flow in 2012 was less than half the typical amount in the 1930s (Gungle et al., 2017, Figure 31). At Gamez Road, base flow had almost vanished by 2018 and was absent in 2019 (The Nature Conservancy, 2020). The SPV in the study area is becoming a set of sub-basins for which the only significant hydrological connection is summer monsoon floodwater. Separation appears to be complete at the Benson Narrows, close to complete at Gamez Road, and well advanced near Sierra Vista.

Isotope Evolution in Base Flow

Figure 10 is a summary of the isotope compositions in base flow from area 1 to area 5. Three possibilities for isotope evolution relating base flow in the five areas can be postulated. Case A consists in sub-flow originating upstream of each area and forced to the surface above each impermeable rock sill. Progressive downstream increases in ($\delta^{18}O$, δ^2H) along an evaporation trend of slope near 4 may occur if flow is at the surface. Case B consists in mixing of sub-flow from upstream with shallow riparian groundwater recharged from summer floods, possibly resulting in downstream increases in ($\delta^{18}O$, δ^2H), as appears to occur in area 2. Case C is characterized by downstream decreases in ($\delta^{18}O$, δ^2H) as a result of additions of low–($\delta^{18}O$, δ^2H) water originating from the higher, well-watered mountain blocks flanking the river basin. All three mechanisms are likely to operate; isotope data allow the identification of the dominant mechanism in a particular area.

Case A is dominant between the Charleston and Tombstone gauges in area 1, resulting in the evaporation trend observed at the Tombstone gauge (Figure 2). Case B is observed in area 2, where base flow plots between the trends for base flow at the Tombstone gauge and for shallow riparian groundwater (Figures 5 and 10). Case C applies in areas 3 and 5 (Figure 10) and between the Hereford and Lewis Springs gauges in area 1 (Figure 5). Between the Lewis Springs and Charleston gauges, cases A and C appear to operate together. In area 4, case B applies to water contributed from Hot Springs Canyon, and case A applies to groundwater from area 3, but without an isotope evaporation signature (Figure 8).

Mountain-Derived Water

Baillie et al. (2007) and Gungle et al. (2017) determined that shallow riparian groundwater and base flow in gaining reaches of area 1 contain a large fraction of groundwater that can be traced to the Huachuca Mountains on the west flank of the river valley in that area (Figures 1 and 5). In area 5, a simple interpretation might identify base flow and groundwater emerging in Bingham Cienega as evaporated amount-weighted mean winter precipitation from near

Downloaded from http://pubs.geoscienceworld.org/aeg/eeg/article-pdf/26/4/463/5196653/i1078-7275-26-4-463.pdf
by University of Arizona user

2420 masl (Figure 10). Such an interpretation is oversimplified, however, because observed values in tributary surface water (Figure 9), base flow, and water in the cienega are likely to be mixtures of water from Edgar and Buehman Canyons. Water in Edgar Canyon is evaporated relative to the LMWL defined by the amount-weighted seasonal means for 2420 masl, and it would originate from precipitation with ($\delta^{18}O$, $\delta^{2}H$) values lower than those of mean winter precipitation. The data for base flow in Edgar Canyon represent the years 1998, 1999, 2001, and 2012 and are therefore unlikely to be influenced by individual seasons with low–($\delta^{18}O$, $\delta^{2}H$) precipitation. Cunningham et al. (1998) observed comparable low ($\delta^{18}O$, $\delta^{2}H$) values in the discharge of springs between 1400 and 2000 masl. The reason for preferential infiltration of water with ($\delta^{18}O$, $\delta^{2}H$) values lower than those of average winter precipitation is not understood; it is not an isotope effect related to the amount or monthly intensity of high-elevation precipitation (Eastoe and Wright, 2019).

Area 1

Base flow in area 1 is dependent partly on discharge from a sub-basin in Mexico, south of Palominas (Pool and Dickinson, 2007, Figure 2), and partly on discharge from the alluvial aquifer between the Huachuca Mountains and the SPR, focused between Hereford and Lewis Springs (Figure 5). The latter groundwater flows east from the Huachuca Mountains (Pool and Dickinson, 2007, Figure 5) and originates largely as precipitation in the mountains (Wahi et al., 2008).

Area 2

Sources of base flow in area 2 are: (1) bank storage, mainly recharge from summer floodwater, (2) discharge from area 1, (3) and (4) discharge from the confined aquifer beneath the Benson Clay (Figure 6). The relative importance of the sources cannot be established from the isotope data. Two riverbed discharge zones of confined groundwater have been found; others may exist in the area, or they may have existed prior to intensive pumping of the confined aquifer at St. David. The temporal change in isotope content at Seeps A from confined-aquifer to bank-storage discharge (Figure 6) indicates that the head driving discharge from the confined aquifer is at times exceeded by the head of water in the river during summer floods, leading to recharge rather than discharge.

Area 3

Base flow in area 3 might also be interpreted in three alternative ways: (1) as evaporated winter precipitation from 2420 masl (indicated by the line of slope 4 in Figure 10), (2) as a mixture of confined and shallow riparian groundwater from upstream of the Benson Narrows (Figure 7), or (3) as groundwater originating from the watershed of Red Rock Creek. Alternative (1) is not reasonable because the watershed of Red Rock Creek is mainly at altitudes of 1150–1400 masl, with a small area near 1600 masl. Alternative (2) would require about-equal proportions of the confined and shallow riparian groundwater, but it lacks a means to transfer water across the granite sill separating the sub-basins. No base flow was observed in the riverbed from 2006 to 2009 when a stream gauge was operated at the sill (U.S. Geological Survey, 2019) or since (personal observation). Haney and Lombard (2005) proposed that groundwater from the sub-basin upstream of the granite sill flows through alluvium to the east and west of the granite hills in the area. Drewes (1974) constructed a cross section across the SPV at the Benson Narrows, showing a granite barrier extending continuously across the valley, locally capped by alluvium deposited on a surface that lies slightly higher than the riverbed. If this is correct in detail, confined and shallow riparian groundwater leaves the upstream sub-basin along the river channel, and only unconfined groundwater from alluvium along the basin flanks could flow around the granite sill. Alternative (3) is favored by the spatial association of base flow with Red Rock Creek and the close isotopic similarity between the base flow at site TLC and other groundwater of local origin in the sub-basin below the Benson Narrows (Eastoe and Clark, 2018).

Red Rock Creek is unusual in generating a perennial reach of the river. Kelsey and Teran Washes, which drain watersheds of comparable size and elevation, do not generate perennial flow in the river, even though impermeable clay is present in the riverbed near their junctions. This suggests the presence of an unusual groundwater storage in the watershed of Red Rock Creek. Such a storage may be associated with sediment deposited by a major tributary that was located near Red Rock Creek at the time of deposition of the Quiburis Formation. The tributary deposited a large alluvial fan, of which the eroded remnant is visible in the Quiburis Formation (Figure 2).

Area 4

Hot Springs Canyon also supplies enough water to feed seeps in the riverbed. In this instance, much of the sub-flow originating in the canyon derives from a set of hot springs in the upper watershed (Eastoe and Clark, 2018). Groundwater supplied from Hot Springs Canyon is subject to pumping for irrigation

Downloaded from http://pubs.geoscienceworld.org/aeg/eeg/article-pdf/26/4/463/5196653/i1078-7275-26-4-463.pdf
by University of Arizona user

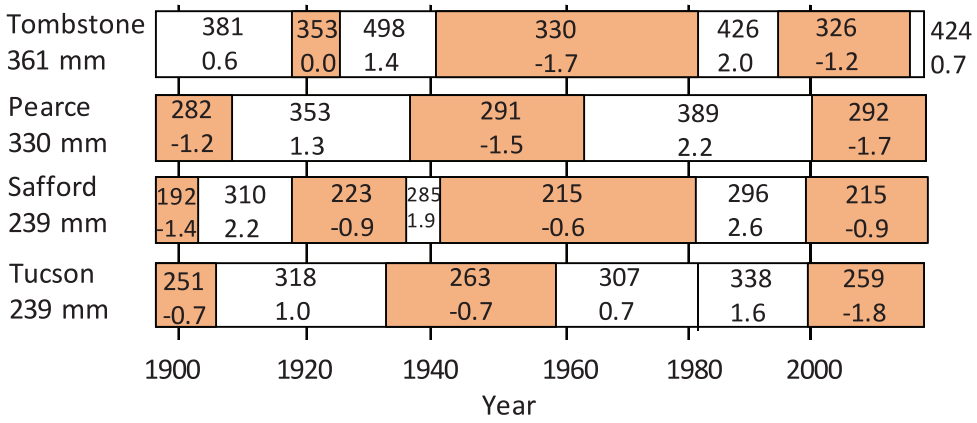

Figure 11. Drought status at four stations in southeastern Arizona, from 1896 to present. Shading indicates drought conditions, and white indicates non-drought conditions, as indicated by annual average precipitation (upper figure) and the Palmer Drought Severity Index (lower figure), both averaged over the time interval indicated by each box. Long-term average precipitation is given below each site name. Data are from WestWide Drought Tracker, 2019, 2–10). Site locations are: Tombstone (31.7147°N, 110.0659°W), Pearce (31.9410°N, 109.8363°W), Safford (32.8149°N, 109.6804°W), Tucson (32.1242°N, 110.9403°W).

immediately up-gradient of the seeps; prior to development, this aquifer may have supplied a larger fraction of base flow in area 4.

Area 5

At Bingham Cienega, the following hypothesis (illustrated in Figure 2) is proposed for the origin of groundwater and former base flow in the adjacent SPR. Both Edgar and Buehman Canyons cross east-dipping limestone of the Pennsylvanian–Permian Naco Group. The limestone is overlain unconformably by Cretaceous Bisbee Group strata, largely shale and phyllite, in the area near Edgar Canyon (Bykerk-Kaufmann, 1990). Recharge into limestone occurs beneath both canyons, and groundwater flows east through the tilted limestone strata. Over much of the area, the groundwater is confined beneath the Bisbee Group. At the fault bounding the relatively impermeable lacustrine basin-fill sediments of the SPV, the groundwater flows upwards along the fault, and discharge is focused near Bingham Cienega. Flow through the karst aquifer is rapid, as indicated by the tritium measurements in 2001 (Supplemental Table S1). The aquifer supplying Bingham Cienega and perennial flow in the nearby reach of the SPR are therefore vulnerable to drought at decadal or shorter timescales. Discharge was plentiful in the cienega prior to the early 2000s, and base flow was present in the river. Subsequently, discharge has been largely absent. The change probably reflects a regional change from relatively wet years to drought in the late 1990s (Figure 11).

Natural or Human Causes

At Charleston, a steady decline in base flow has been documented over the period 1934–2012 (Gungle et al., 2017). Long-term drought conditions began in the 1940s at the nearby climate station in Tombstone; between 1941 and 2019, negative Palmer Drought Severity Index values indicative of drought applied in 56 of 78 years (Figure 11; data from WestWide Drought Tracker, 2019). Intervals of drought in neighboring areas of southeastern Arizona have not corresponded exactly to those in Tombstone and may not correspond in other parts of the SPV. Further indications of long-term drought in the SPV are found in the alluvial aquifer in Hot Springs Canyon, Cascabel (Figure 2), where pumping demands are small, and where long-term declines in groundwater levels have been documented since 1993 (Eastoe and Clark, 2018). Similar declines have been observed in several, but not all, mountain-front wells in the area near Benson and Cascabel (Cordova et al., 2015).

Climate in southwest North America was wetter during the Little Ice Age. At the peak of the Little Ice Age, extensive standing water was present in Lake Palomas, Chihuahua, in a basin that is typically dry at present (Castiglia and Fawcett, 2006). Silver Lake in the Mojave River drainage, southern California system, was flooded at 390 ± 90 years before present but is at present typically dry (Enzel et al., 1989). Large floods were more common than at present in Arizona streams during an interval of wet climate beginning about A.D. 1400 (Ely, 1997), and ending since A.D. 1650 at a time that cannot be constrained

Downloaded from http://pubs.geoscienceworld.org/aeg/eeg/article-pdf/26/4/463/5196653/i1078-7275-26-4-463.pdf
by University of Arizona user

precisely from calibrated radiocarbon dates because of cyclic fluctuations in the production rate of ^{14}C between A.D. 1650 and 1950 (Stuiver and Becker, 1993). Nonetheless, a drying trend is likely since A.D. 1800.

Natural drying at decadal to centennial timescales in the SPV has been exacerbated by human exploitation of groundwater, and it may be further affected by human-caused climate change. Demand for groundwater declined between 1970 and 2010 across the SPV as a result of retirement of irrigated agricultural land and increased water-use efficiency in Sierra Vista; nonetheless, estimated outflow exceeded inflow in the Sierra Vista, Benson, and Cascabel-Redington sub-basins of the SPV (for sub-basins as defined in their works, see Cordova et al., 2015; Gungle et al., 2017). In all three sub-basins, human demand takes up a large fraction of estimated inflow (Table 1). Errors in the water budgets are large, especially for the evapotranspiration component of outflow. In the case of Sierra Vista sub-basin, the imbalance between inflow and outflow in 2012 was estimated with an error at -6.2 ± 6.8 hm^3/yr. Errors notwithstanding, human demand in the Sierra Vista sub-basin is very likely unsustainable at present, and it was clearly unsustainable in 2002, when the imbalance was -13.3 ± 6.8 hm^3/yr (Gungle et al., 2017). Declining base flow in the SPR is therefore most likely an effect of persistent drought combined with human demand for groundwater, even as human demand has decreased.

Implications for Management of the SPV

The sub-basins of the SPV will become increasingly reliant on local water sources, i.e., surface water and groundwater supplied by tributaries, as their hydrological separation develops. Groundwater in areas 3 and 4, within the sub-basin downstream of the Benson Narrows, will be little affected by additional pumping in area 2, upstream of Benson Narrows. Declining water levels in area 2 have already separated the two sub-basins. Within areas 3 and 4, the future of perennial flow in the SPR and groundwater supply will be dominantly affected by climate and by local pumping. Monsoon floodwater appears to have little role in recharge in these areas.

In area 1, delayed effects of pumping to date are likely to cause capture of some of the river flow, regardless of future measures to manage groundwater (Gungle et al., 2017). Artificial recharge of stormwater from the City of Sierra Vista is an attempt at capturing the abundant summer runoff that otherwise contributes little to recharge beyond losing reaches of the riparian zone (Figure 4; Baillie et al., 2007). Low-density urban development south of Sierra Vista relies on private supply wells for water pumped from the regional aquifer, competing for water that would otherwise discharge into the reach between Hereford and Lewis Springs. Increased density of urban development south of Sierra Vista will combine with the effects of drought to reduce the volume of base flow in the river.

In area 2, any lessening of the confined-aquifer head as a result of increased pumping for proposed urban development near Benson risks permanently reversing the discharge of confined-aquifer groundwater in and near the SPR near St. David. Over-pumping causes long-lasting changes in artesian aquifers, as in the case of the Roswell Basin, New Mexico, where over-exploitation of groundwater has decreased the head of formerly artesian groundwater by tens of meters (Havenor, 1996). In area 2, likely effects of over-exploitation include reversal of groundwater flow from the confined aquifer, draining of shallow riparian groundwater from the riverbed alluvium, reduction or elimination of perennial flow in in the river, and drying of the St. David Cienega. A change in head of 1–2 m (typical floodwater depth) may be enough to reverse the direction of groundwater flow, on the indication of changes in isotope composition of the seeps at Escalante Crossing. Loss of perennial flow in this area would eliminate the only dependable source of surface water between the Tombstone gauge and Red Rock Creek, a distance of 65 km.

In areas 3 and 4, long-term decline in base flow reflects a combination of pumping and drought effects as observed in Hot Springs Canyon (Eastoe and Clark, 2018). Drought-related drainage of groundwater above the level of the SPR in tributary washes is likely to be a regional phenomenon. The retirement of irrigated land in area 3 (Haney and Lombard, 2005) has no doubt slowed the shortening of the perennial reach in that area but cannot address drought as a factor contributing to the decline of groundwater discharge. In area 4, the effects of drought-related drainage from Hot Springs Canyon will probably take several decades to reach the declining perennial reach, on the indication of tritium data (Eastoe and Clark, 2018). Perennial flow in this reach will also depend on the supply of groundwater from area 3, with a similar lag time relative to drought and pumping demand.

In area 5, both the SPR and Bingham Cienega are expected respond to climate fluctuations. If the interpretation of groundwater origin in area 5 is correct, the presence of base flow in the SPR and groundwater discharge to Bingham Cienega will depend on climate changes at decadal or shorter timescales, and will be little affected by pumping for irrigation along the SPR upstream of Bingham Cienega.

Downloaded from http://pubs.geoscienceworld.org/aeg/eeg/article-pdf/26/4/463/5196653/i1078-7275-26-4-463.pdf
by University of Arizona user

Future Work

Area 1 has been studied in greater detail than areas 2 to 5 because of its ecological importance and because of its high degree of urban development. Further study of areas 2 to 5 would improve the interpretations presented here. Area 2 is of particular importance because of proposals for urban development equal to that in area 1.

CONCLUSIONS

1. Four reaches of the SPR in the study area currently have ecologically important base flow. A fifth reach, near Redington, had base flow until the early 2000s. Base flow in the SPR is declining, both in volume and in the lengths of river reaches with perennial flow.
2. The SPV in the study area comprises four subbasins separated by impermeable rock sills at the level of the river. Base flow crosses sills near Sierra Vista and north of Cascabel near Gamez Road, but it has almost disappeared in the latter case. No base flow crosses the Benson Narrows sill at present.
3. Recharge in losing reaches of the SPR from summer floodwater results in bank storage and shallow riparian groundwater with stable O and H isotope data forming an evaporation trend.
4. In area 1, south of Sierra Vista, stable O and H isotope data indicate addition of alluvial basin groundwater originating in the Huachuca Mountains to SPR base flow.
5. In area 2, near St. David, base flow is a combination of water from area 1, local bank storage, and deep-basin groundwater. Small changes of head in the deep-basin groundwater in this area will result in reversal of groundwater flow and recharge to the deep-basin aquifer from the riverbed.
6. In area 3, north of the Benson Narrows, stable O and H isotope and tritium data suggest that base flow originates from a local tributary drainage rather than upstream in the SPV.
7. In area 4, in Cascabel near Gamez Road, a single base-flow sample indicated a water origin mainly in the SPV alluvial aquifer immediately upstream. Riverbed seeps also contribute water from Hot Springs Canyon.
8. In area 5, near Redington, former base flow originated as precipitation from neighboring high mountains, and it was apparently supplied to the riverbed through a limestone aquifer. Tritium data are consistent with transit times of a few years and indicate the vulnerability of this reach and nearby wetlands to short-term drought.
9. High human demand for groundwater in the SPV in recent decades has coincided with a period of dry climate at decadal to centennial timescale. Lessening agricultural demand for groundwater since 1970 has not yet resulted in observable recovery of base flow in the SPR. Large additional human demands for groundwater will exacerbate the decline of base flow.

SUPPLEMENTAL MATERIAL

Supplemental Material associated with this article can be found online at https://doi.org/10.2113/EEG-xxxx.

ACKNOWLEDGMENTS

The author expresses his gratitude to: Pima County Regional Flood Control District and Pima Association of Governments for permission to use their data from the Bingham Cienega area, and to Pima County employees Jennifer Becker, Brian Powell, Julia Fonseca, and Gregory Hess for assistance in sampling; Apache Nitrogen Products, Inc., employees Greg Hall for assistance with sampling and Pamela Beilke for permission to use data; Mary McCool and the Community Watershed Alliance for organizing sampling at St. David Cienega; the Cascabel community for access to their property and private wells; Robert Rogers and Barbara Clark of The Nature Conservancy for access to a river sampling site and assistance with sampling in Cascabel; Bureau of Land Management employees David Murray and Benjamin Lomeli for access to the San Pedro Riparian National Conservation Area; and Lynwood Hume for collecting floodwater samples in Cascabel when the author was unable to be present. The input of two anonymous reviewers helped greatly in improving the quality of the manuscript.

REFERENCES

Abatzoglou, J. T.; McEvoy, D. J.; and Redmond, K. T., 2017, The West Wide Drought Tracker: Drought monitoring at fine spatial scales: *Bulletin American Meteorological Society*, Vol. 98, No. 9, pp. 1815–1820.

Arizona Daily Star, 2016, *Mega-Project in Benson Casting Shadow over Kartchner Caverns Water Supply*: Electronic document, available at https://azdailysun.com/news/local/mega-project-in-benson-casting-shadow-over-kartchner-caverns-water/article_4b88974e-753e-52e0-ad8a-bebef18e0a12.html

Baillie, M. N.; Hogan, J. F.; Ekwurzel, B.; Wahi, A. K.; and Eastoe, C. J., 2007, Quantifying water sources to a semiarid riparian ecosystem, San Pedro River, Arizona: *Journal Geophysical Research*, Vol. 112, G03S02. doi:10.1029/2006JG000263.

Beilke, P., Apache Nitrogen Products Inc., Benson, AZ, personal communication.

Blumstock, M.; Tetzlaff, D.; Malcolm, I. A.; Nuetzmann, G.; and Soulsby, C., 2015, Baseflow dynamics: Multi-tracer surveys to assess variable groundwater contributions to mon-

Downloaded from http://pubs.geoscienceworld.org/aeg/eeg/article-pdf/26/4/463/5196653/i1078-7275-26-4-463.pdf
by University of Arizona user

tane streams under low flows: *Journal Hydrology*, Vol. 527, pp. 1021–1033.

Brand, L. A.; Cerasale, D. J.; Rich, T. O.; and Krueper, D. J., 2009, Breeding and migratory birds: Patterns and processes. In Stromberg, J. C. and Tellman, B. (Editors), *Ecology and Conservation of the San Pedro River*: The University of Arizona Press, Tucson, AZ, pp. 153–174.

Brooks, J. R.; Wigington, J.; Phillips, D. L.; Comeleo, R.; and Coulombe, R., 2012, Willamette River Basin surface water isoscape (delta O-18 and delta H-2): Temporal changes of source water within the river: *Ecosphere*, Vol. 3, No. 5, article 39. doi:10.1890/es11-00338.1.

Bryan, K., 1925, Date of channel entrenching (arroyo cutting) in the arid southwest: *Science*, Vol. 62, No. 1607, pp. 338–344.

Bykerk-Kaufmann, A., 1990, *Kinematic Analysis of Deformation at the Margin of a Regional Shear Zone, Buehman Canyon Area, Santa Catalina Mountains, Arizona*: *Unpublished M.S. Thesis*, Department of Geosciences, University of Arizona, Tucson, AZ, 79 p.

Castiglia, P. J. and Fawcett, P. F., 2006, Large Holocene lakes and climate change in the Chihuahuan desert: *Geology*, Vol. 34, No. 2, pp. 113–116.

Coes, A. L. and Pool, D. R., 2007, Ephemeral-stream channel and basin-floor infiltration and recharge in the Sierra Vista subwatershed of the Upper San Pedro Basin, southeastern Arizona. In Stonestrom, D. A.; Constantz, J.; Ferre, T.; and Leake, S. A. (Editors), *Ground-Water Recharge in the Arid and Semiarid Southwestern United States*: U.S. Geological Survey Professional Paper 1703-J, pp. 253–311.

Cook, J. P.; Youberg, A.; Pearthree, P. A.; Onken, J. A.; MacFarlane, B. J.; Hadad, D. E.; Bigio, E. R.; and Kowler, A. L., 2010, *Mapping of the Holocene River Alluvium Along the San Pedro River, Aravaipa Creek, and Babocomari River, Southeastern Arizona*: Arizona Geological Survey Digital Map DM-RM-1, 76 p.

Cordova, J. T.; Dickinson, J. E.; Beisner, K. R.; Hopkins, C. B.; Kennedy, J. R.; Pool, D. R.; Glenn, E. P.; Nagler, P. L.; and Thomas, B. E., 2015, *Hydrology of the Middle San Pedro Watershed, Southeastern Arizona*: *U.S. Geological Survey Scientific Investigations Report 2013-5040*, 77 p.

Cunningham, E. E. B.; Long, A.; Eastoe, C. J.; and Bassett, R. L., 1998, Migration of recharge waters downgradient from the Santa Catalina Mountains into the Tucson Basin aquifer: *Hydrogeology Journal*, Vol. 6, No. 1, pp. 94–103.

Dickinson, J. E.; Kennedy, J. R.; Pool, D. R.; Cordova, J. T.; Parker, J. T. C.; Macy, J. P.; and Thomas, B. E., 2010a, *Hydrogeologic Framework of the Middle San Pedro Watershed, Southeastern Arizona*: *U.S. Geological Survey Scientific Investigations Report 2010–5126*, 36 p.

Dickinson, J. E.; Pool, D. R.; Groom, R. W.; and Davis, L. J., 2010b, Inference of lithologic distributions in an alluvial aquifer using airborne transient electromagnetic surveys: *Geophysics*, Vol. 75, No. 4, p. WA149–WA161.

Dickinson, W. R., 1991, *Tectonic Setting of Faulted Tertiary Strata Associated with the Catalina Core Complex in Southern Arizona*: Special Paper 264, Geological Society of America, Boulder, CO, 106 p.

Dickinson, W. R., 1998, *Facies Map of Post–Mid-Miocene Quiburis Formation, San Pedro Trough, Pinal, Pima, Gila, Graham, and Cochise Counties, Arizona*: Arizona Geological Survey Contributed Map CM-98-A, map scale 1:24,000, 10 map sheets.

Dickinson, W. R., 2002, The Basin and Range Province as a composite extensional domain: *International Geology Review*, Vol. 44, No. 1, pp. 1–38.

Dickinson, W. R., 2003, Depositional facies of the Quiburis Formation, basin fill of the San Pedro trough, southeastern Arizona Basin and Range Province. In Raynolds, R. G. and Flores, R. M. (Editors), *Cenozoic Systems of the Rocky Mountain Region*: Society for Sedimentary Geology, Denver, CO, pp. 157–181.

Drewes, H., 1974, *Geologic Map and Sections of the Happy Valley Quadrangle, Cochise County, Arizona*: U.S. Geological Survey Miscellaneous Investigations Series Map I-832, 1 sheet, scale 1:48,000.

Eastoe, C. J. and Clark, B., 2018, Understanding the water resources of a small rural community: Citizen science in Cascabel, Arizona: *Journal Contemporary Water Research and Education*, Vol. 164, pp. 19–41.

Eastoe, C. J. and Dettman, D. L., 2016, Isotope amount effects in hydrologic and climate reconstructions of monsoon climates: Implications of some long-term data sets for precipitation: *Chemical Geology*, Vol. 430, pp. 76–89.

Eastoe, C. J. and Towne, D., 2018, Regional zonation of groundwater recharge mechanisms in alluvial basins of Arizona: Interpretation of isotope mapping: *Journal Geochemical Exploration*, Vol. 194, pp. 134–145.

Eastoe, C. J.; Watts, C. J.; Ploughe, M.; and Wright, W. E., 2011, Future use of tritium in mapping pre-bomb groundwater volumes: *Ground Water*, Vol. 50, pp. 87–93.

Eastoe, C. J.; and Wright, W. E., 2019, Hydrology of mountain blocks in Arizona and New Mexico as revealed by isotopes in groundwater and precipitation: *Geosciences*, Vol. 9, article 461. doi:10.3390/geosciences9110461.

Ely, L. L., 1997, Response of extreme floods in the southwestern United States to climatic variations in the late Holocene: *Geomorphology*, Vol. 19, No. 3, pp. 175–201.

Enzel, Y.; Cayant, D. R.; Anderson, R. Y.; and Wels, S. G., 1989, Atmospheric circulation during Holocene lake stands in the Mojave Desert: Evidence of regional climate change: *Nature*, Vol. 341, No. 6237, pp. 44–47.

Fenneman, N. M., 1931, *Physiography of Western United States*, 1st ed.: McGraw-Hill, New York, NY, 534 p.

Fujimoto, M.; Ohte, N.; Kawasaki, M.; Osaka, K.; Itoh, M.; Ohtsuka, I.; and Itoh, M., 2016, Influence of bedrock groundwater on streamflow characteristics in a volcanic catchment: *Hydrological Processes*, Vol. 30, No. 4, pp. 558–572.

Glenn, E. P.; Scott, R. L.; Nguyen, U.; and Nagler, P. L., 2015, Wide-area ratios of evapotranspiration to precipitation in monsoon-dependent semiarid vegetation communities: *Journal Arid Environments*, Vol. 117, pp. 84–95.

Gray, R. S., 1965, *Late Cenozoic Sediments in the San Pedro Valley near St. David, Arizona*: *Unpublished M.S. Thesis*, University of Arizona, Tucson, AZ, 198 p.

Guay, B. E.; Eastoe, C. J.; Bassett, R. L.; and Long, A., 2006, Sources of surface and ground water adjoining the Lower Colorado River inferred by $\delta^{18}O$, δD and ^{3}H: *Hydrogeology Journal*, Vol. 14, No. 4, pp. 146–188.

Gungle, B. G.; Callegary, J. B.; Paretti, N. V.; Kennedy, J. R.; Eastoe, C. J.; Turner, D. S.; Dickinson, J. E.; Levick, L. R.; and Sugg, Z. P., 2017, *Hydrological Conditions and Evaluation of Sustainable Groundwater Use in the Sierra Vista Subwatershed, Upper San Pedro Basin, Southeastern Arizona*: *U.S. Geological Survey Scientific Investigation Report 2016–5114*, 90 p.

Haney, J. and Lombard, J., 2005, Interbasin groundwater flow at the Benson Narrows, Arizona: *Southwest Hydrology*, March/April issue, pp. 8–9.

Havenor, K. C., 1996, *The Hydrogeologic Framework of the Roswell Groundwater Basin, Chaves, Eddy, Lincoln, and Otero*

Downloaded from http://pubs.geoscienceworld.org/aeg/eeg/article-pdf/26/4/463/5196653/i1078-7275-26-4-463.pdf
by University of Arizona user

Counties, New Mexico: *Unpublished Ph.D. thesis*, Department of Geosciences, University of Arizona, Tucson, AZ, 274 p.

Hereford, R. and Betancourt, J., 2009, Historic geomorphology of the San Pedro River. In Stromberg, J. C. and Tellman, B. (Editors), *Ecology and Conservation of the San Pedro River*: The University of Arizona Press, Tucson, AZ, pp. 232–250.

Hogan, J.; Phillips, F.; Eastoe, C.; Lacey, H.; Mills, S.; and Oelsner, G., 2012, Isotopic tracing of hydrological processes and water quality along the upper Rio Grande, USA. In *Monitoring Isotopes in Rivers: Creation of the Global Network of Isotopes in Rivers (GNIR)*: Tecdoc 1673, International Atomic Energy Agency, Vienna, Austria, pp. 111–136.

Hopkins, C.; McIntosh, J.; Eastoe, C.; Dickinson, J. E.; and Meixner, T., 2014, Evaluation of the importance of clay confining units on groundwater flow in alluvial basins using solute and isotope tracers: The case of Middle San Pedro Basin in southeastern Arizona (USA): *Hydrogeology Journal*, Vol. 22, No. 4, pp. 829–849. doi:10.1007/s10040-013-1090-0.

Huckleberry, G.; Lite, S. T.; Katz, G.; and Pearthree, P., 2009, Fluvial geomorphology. In Stromberg, J. C. and Tellman, B. (Editors), *Ecology and Conservation of the San Pedro River*: The University of Arizona Press, Tucson, AZ, pp. 251–267.

Hughes, C. E.; Stone, D. J. M.; Gibson, J. J.; Meredith, K. T.; Sadek, M. A.; Cendon, D. I.; Hankin, S. I.; Hollins, S. E.; and Morrison, T. N., 2012, Stable water isotope investigation of the Barwon–Darling River system, Australia. In *Monitoring Isotopes in Rivers: Creation of the Global Network of Isotopes in Rivers (GNIR)*: Tecdoc 1673, International Atomic Energy Agency, Vienna, Austria, pp. 95–110.

MacNish, R.; Baird, K. J.; and Maddock, T., 2009, Groundwater hydrology of the San Pedro River Basin. In Stromberg, J. C. and Tellman, B. (Editors), *Ecology and Conservation of the San Pedro River*: The University of Arizona Press, Tucson, AZ, pp. 285–299.

Maricopa Audubon Society, 2020, *Birds of San Pedro Riparian National Conservation Area*: Electronic document, available at https://www.maricopaaudubon.org/bird-checklist-for-san-pedro-riparian-national-conservation-area

Nickolas, L. B.; Segura, C.; and Brooks, J. R., 2017, The influence of lithology on surface water sources: *Hydrological Processes*, Vol. 31, No. 10, pp. 1913–1925.

Pfister, L.; Martinez-Carreras, N.; Hissler, C.; Klaus, J.; Carrer, G. E.; Stewart, M. K.; and McDonnell, J. J., 2017, Bedrock geology controls on catchment storage, mixing, and release: A comparative analysis of 16 nested catchments: *Hydrological Processes*, Vol. 31, No. 10, pp. 1828–1845.

Phillips, F. M.; Mills, S.; Hendrickx, M. H.; and Hogan, J., 2003, Environmental tracers applied to quantifying causes of salinity in arid-region rivers: Results from the Rio Grande Basin, southwestern USA: *Developments in Water Science*, Vol. 50, pp. 327–334.

Pool, D. and Dickinson, J. E., 2007, *Ground-Water Flow Model of the Sierra Vista Subwatershed and Sonoran Portions of the Upper San Pedro Basin, Southeastern Arizona, United States, and Northern Sonora, Mexico*: *U.S. Geological Survey Scientific Investigations Report 2006-5228*, 48 p.

Rosen, P. C., 2009, Reptiles and amphibians. In Stromberg, J. C. and Tellman, B. (Editors), *Ecology and Conservation of the San Pedro River*: The University of Arizona Press, Tucson, AZ, pp. 175–191.

Segura, C.; Noone, D.; Warren, D.; Jones, J.; Tenney, J.; and Ganio, L., 2019, Climate, landforms, and geology affect baseflow sources in a mountain catchment: *Water Resources Research*, Vol. 55, No. 7, pp. 5238–5254.

Singh, N. K.; Emanuel, R. E.; and McGlynn, B. L., 2016, Variability in isotopic composition of base flow in two headwater streams of the southern Appalachians: *Water Resources Research*, Vol. 52, No. 6, pp. 4264–4279.

Soulsby, C.; Malcolm, R.; Helliwell, R.; Ferrier, R. C.; and Jenkins, A., 2000, Isotope hydrology of the Allt a' Mharcaidh catchment, Cairngorms, Scotland: Implications for hydrological pathways and residence times: *Hydrological Processes*, Vol. 14, No. 4, pp. 747–762.

Soycan, C. U.; Brand, L. A.; and Saba, J. I., 2009, Causes and consequences of mammal species richness. In Stromberg, J. C. and Tellman, B. (Editors), *Ecology and Conservation of the San Pedro River*: The University of Arizona Press, Tucson, AZ, pp. 107–126.

Stuiver, M. and Becker, B., 1993, High-precision decadal calibration of the radiocarbon time scale, AD 1950–6000 BC: *Radiocarbon*, Vol. 35, No. 1, pp. 35–66.

Tague, C. and Grant, G. E., 2004, A geological framework for interpreting the low-flow regimes of Cascade streams, Willamette River Basin, Oregon: *Water Resources Research*, Vol. 40, No. 4, W04303.

Tetzlaff, D. and Soulsby, C., 2008, Sources of baseflow in larger catchments—Using tracers to develop a holistic understanding of runoff generation: *Journal Hydrology*, Vol. 359, pp. 287–302.

The Nature Conservancy, 2020, *San Pedro River Wet-Dry Maps*: Electronic document, available at http://azconservation.org/downloads/san_pedro_wet_dry_mapping

U.S. Geological Survey, 2019, *National Water Information System, Web Interface, USGS 09471800 San Pedro River near Benson, Ariz.*: Electronic document, available at https://nwis.waterdata.usgs.gov/az/nwis/uv?cb_00060=on&format=gif_default&site_no=09471800&

Wahi, A. K.; Hogan, J. F.; Ekwurzel, B.; Baillie, M. N.; and Eastoe, C. J., 2008, Geochemical quantification of semiarid mountain recharge: *Ground Water*, Vol. 46, pp. 414–425.

Waters, M. R. and Haynes, C. V., 2001, Late Quaternary arroyo formation and climate change in the American Southwest: *Geology*, Vol. 29, No. 5, pp. 399–402.

Western Regional Climate Center, 2019, *Coop Sites Arizona*: Electronic document, available at http://www.wrcc.dri.edu/summary/Climsmaz.html

WestWide Drought Tracker, 2019, *WestWide DroughtTracker*: Electronic document, available at https://wrcc.dri.edu/wwdt/time/

Downloaded from http://pubs.geoscienceworld.org/aeg/eeg/article-pdf/26/4/463/5196653/i1078-7275-26-4-463.pdf
by University of Arizona user

Downloaded from http://pubs.geoscienceworld.org/aeg/eeg/article-pdf/26/4/463/5196653/i1078-7275-26-4-463.pdf
by University of Arizona user